Journal of Applied Electrochemistry **31**: 935–940, 2001.

Characterization of electrodeposited thin layers of magnetic alloys by Mössbauer spectroscopy

C. LICOUR[1], A. GÉRARD[2], C. JÉRÔME[3], L. RABET[4] and L. MARTINOT[1,*]
[1]*Coordination Chemistry and Radiochemistry, University of Liège, B16 Sart-Tilman, B-4000 Liège, Belgium*
[2]*Laboratory of Solid Physics, University of Liège, Belgium*
[3]*Centre for Education and Research on Macromolecules (CERM), University of Liège, Belgium*
[4]*Royal Military School, Brussels, Belgium*
*(*Research Associate of the Inter-University Institute for Nuclear Sciences, Brussels)*

Received 30 May 2000; accepted in revised form 13 February 2001

Key words: deposition, magnetic properties, Mössbauer spectroscopy, rare earths

Abstract

Rare earth and transition metal alloys are interesting magnetic materials for applications in the field of magnetooptical memories. We describe the preparation of Dy/Fe alloys by electrodeposition using a pulsed galvanostatic process. Samples were characterized by Mössbauer spectroscopy. Thin layers obtained with short electrolysis pulses (0.1 s) give a Mössbauer spectrum analysed as the sum of two subspectra: the first corresponds to a spectrum originating from very small sized particles of Fe and the second is attributed to a Dy/Fe phase. Longer electrolysis pulses (1 s) give samples whose spectrum is also the sum of two subspectra: the first is attributed to metallic Fe with an extended particle-size distribution while the second is attributed to a Fe/Dy alloy. Mössbauer spectroscopy was found useful in determining the best electrolysis parameters leading to domains of uniform magnetization with high coercive fields.

1. Introduction

Alloys based on a rare earth (RE) and a transition metal (TM) are known as useful magnetic materials for the production of magnetooptical memories with high remanent magnetic inductions and high coercive fields [1]. If iron is used as a transition metal, Mössbauer spectroscopy (MS) is a valuable tool for characterization of the magnetic properties [2, 3]. The magnetic hyperfine splitting of the spectrum, theoretically a sextuplet, gives information concerning the hyperfine field (HF) at the iron nucleus and, therefore, on the magnetic field at the iron atom. The relative intensities of the peaks of this sextuplet enable the orientation of the magnetic moments to be determined. Such magnetic compounds are usually prepared by vacuum evaporation or glow discharge sputtering [1, 4, 5]. The magnetic susceptibility and the hysteresis loops of these materials have been reported [4, 5].

Electrodeposition of magnetic alloys consisting of a RE and a TM, in nonaqueous solvents, is an alternative way of obtaining thin layer deposits. Some alloys, Dy/Fe, Sm/Co, Gd/Co, have been electrodeposited in various organic media [6–9]. Several parameters such as the electrochemical bath composition and the cathodic current density have been investigated but only a few hysteresis loops have been published, revealing low values of coercive field [6, 8].

This paper deals with the synthesis of Dy/Fe magnetic alloys in formamide by pulsed galvanostatic deposition. We use diamagnetic cathodes (copper and gold) but we previously deposited magnetic alloys onto conducting polymers [10]. Cyclic voltammetry (CV) was involved to optimize electrolysis parameters while hysteresis loop recordings and MS helped to define the best electrochemical parameters required to obtain magnetic compounds.

Scanning electron microscopy coupled with an energy dispersive X-ray analyser (SEM/EDXA) was used for the analyses of the deposits.

2. Experimental details

Solutions were prepared according to the procedure reported by Matsuda et al. [7]. Formamide (Acros, PA) was dried on 3 Å molecular sieve for 24 h and then distilled under dynamic vacuum. Hydrated dysprosium chloride ($DyCl_3.6\ H_2O$, Alfa 99.9%) and ferrous chloride ($FeCl_2.4\ H_2O$, Aldrich 99.9%) were used as received and dissolved with the molar ratio 40% Dy to 60% Fe. Total cationic concentration was 0.1 M in all

cases. These solutions were slowly dried on a column of 3 Å molecular sieve for 12 h. The residual water was determined by a Karl-Fischer titration. In solutions containing only $DyCl_3$, the residual water amounted to 80 ppm, but, as ferrous iron disturbs the measurement of water by this technique (probably due to the reversible character of the ferric/ferrous couple), the exact water amount remained unknown for the $DyCl_3$/$FeCl_2$ solutions.

Cyclic voltammetry was carried out with an EG&G M270 potentiostat using a single three-electrode compartment cell of which the cathode was a Pt wire and the anode, as well as the pseudoreference electrode, were Pt sheets.

In the case of electrosyntheses, a three-compartment cell was utilized. The central compartment with the cathode (Cu or Au) was separated by glass fritts from the two anodic compartments each fitted with a Fe soluble anode. For the preparation of samples to be investigated by SEM/EDXA and MS, the cathodic materials were Cu (Goodfellow) or Au(Goodfellow) 2.2 cm^2 sheets. Deposits for hysteresis loop recordings were obtained on a Au (Goodfellow) wire (2 mm dia.). Before electrolysis, the metal cathodes were previously cleaned and rinsed in 3 M H_2SO_4, 6 M NH_4OH, H_2O, acetone and heptane.

Electrolyses were conducted in a pulsed galvanostatic mode. The pulse sequence is described in Figure 1. The 'on time' was adjusted at 0.1 s or 1 s and the 'off time' (rest time) was chosen as 1 s in all cases.

Hysteresis loops were recorded on a classical 'home-made' vibrating sample magnetometer. Mössbauer spectra were obtained from a conventional home-made spectrometer fitted with a ^{57}Co source (Rh matrix).

Conversion electron Mössbauer spectra (CEMS) – 300 K, He–CH_4 proportional counter – were registered with alloys deposited on Cu. All spectra were obtained at constant acceleration with a triangular wave mode in the velocity range ± 10 mm s^{-1}. They were fitted with a 'P-fit' adjustment program (least-squares fitting). All isomer shift (IS) values were expressed against α-Fe. The magnitudes of the hyperfine fields (HF) were converted from mm s^{-1} to tesla (33 T = 10.657 mm s^{-1} at room temperature) [11]. The intensity of the Mössbauer spectra was weak, due to the low content of ^{57}Fe (2.19%) in natural iron and to the low amount of deposited mass.

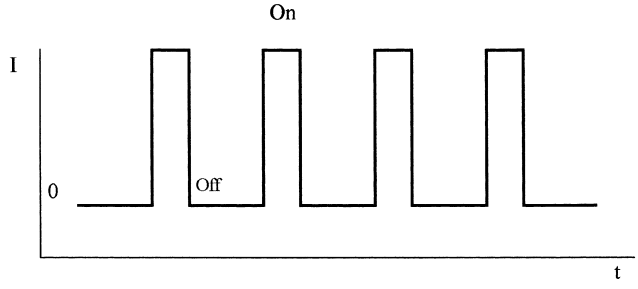

Fig. 1. Cathodic pulse sequence for electrosyntheses.

3. Results

We first investigated by CV the behaviour of the electrolysis bath containing the Dy and Fe salts. The electroactivity window was previously measured with Et_4NClO_4 as a conducting salt. The reduction of the solvent occurs at about −1.5 V against the Pt pseudo-reference. At this potential, gas evolution is noticed and indicator paper (universal indicator paper, UCB) turns violet in this atmosphere, indicating the presence of a gas with basic properties: this is a confirmation of an earlier study [12] which showed the presence of NH_3, as well as that of CO.

Figure 2 shows a typical voltammogram obtained for Dy/Fe solution in formamide. Fe^{2+} is reduced on a Pt cathode at about −1.0 V against the pseudoreference. Under the same conditions, Dy reduction is indicated as a broad shoulder at about –1.7/–2.0 V. At this potential, as mentioned above, solvent reduction already occurs. Crossover of the curves highlights a nucleation phenomenon and therefore, a metallic deposit that dissolves at anodic potentials (anodic peak). The current density (j) measured at −2.0 V reaches 20 mA cm^{-2} and probably corresponds to the reduction of the two cations with simultaneous reduction of the solvent.

Electrolyses were conducted on Cu or Au with the above mentioned bath. Following the recommendation of Matsuda et al. [7], we only used the pulsed galvanostatic technique. A cathodic current intensity higher than 20 mA cm^{-2} was imposed and three values were systematically checked: 30, 40 and 50 mA cm^{-2}, with two pulse sequences: 0.1 s (t_{on})–1 s (t_{off}) and 1 s (t_{on})–1 s (t_{off}). During the t_{on} periods, the cathodic potentials probable range around –2.0 V as expected from

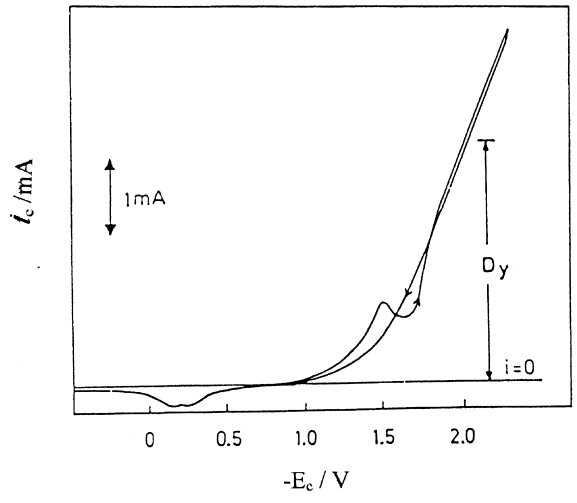

Fig. 2. Cyclic voltammetry curve. Cathode: Pt. Pseudo-reference and auxiliary electrodes: Pt sheets. Bath: 0.06 M $FeCl_2$ and 0.04 M $DyCl_3$ in formamide. Cathodic surface: 0.25 cm^2.

Table 1. Atomic composition of the deposits against the cathodic current density and the pulse sequence

Substrate	Current density /mA cm^{-2}	Pulse sequence /s	Atomic percentage (precision: ±0.2)		
			T.R. (Dy)	M.T. (Fe)	Cl
Cu	30	0.1(on)–1(off)	0.2	99.3	0.5
Au	30	0.1(on)–1(off)	0.8	97.8	1.4
Cu	30	1(on)–1(off)	3.9	80.1	16.0
Cu	40	0.1(on)–1(off)	1.9	97.2	0.9
Au	40	0.1(on)–1(off)	2.1	97.0	0.9
Cu	40	1(on)–1(off)	2.5	93.4	4.1
Cu	50	0.1(on)–1(off)	6.0	93.8	0.2
Au	50	0.1(on)–1(off)	5.8	91.3	2.9
Cu	50	1(on)–1(off)	5.2	94.7	0.1

voltammetric measurements. During the 'off time', the current is experimentally fixed at zero as usual in galvanostatic conditions and the cathode potential has a negative value against the iron soluble anodes. The amount of charge was fixed at 30 C.

As a first step, deposits were characterized by SEM/EDXA to determine their composition and morphology. Table 1 lists the composition of the layers obtained under various conditions.

Results indicate an increasing percentage of RE in the deposit as the cathodic current density increases. The highest content of Dy (6.0%) was attained with a current density of 50 mA cm^{-2}. For lower current densities, the percentage of deposited Dy was lower but Cl was also present in the deposit, probably resulting from $DyCl_3$ precipitation on the cathode. For these lower current densities (30 and 40 mA cm^{-2}), the composition of the alloy is dependent on the length (t_{on}) of the current application, the chlorine content also being enhanced at long t_{on} periods. In spite of the reduction of the solvent, we can conclude that a higher current density enhances the RE content in the alloy.

SEM micrographs reveal acceptable deposits at lower current densities. Figure 3 gives such an example. The morphology of the surface was clearly characterized by a homogeneous and continuous phase containing metallic iron and small inclusions (about 1 μm) of both Fe and Dy. These inclusions were shown to contain 98.8% of Fe and 1.2% of Dy. The visual appearance of these layers is that of a bright metallic surface. Thus, the best system to obtain a sufficient Dy content was pulsed galvanostatic deposition (0.1 s (t_{on})–1 s (t_{off})) with a cathodic current of 50 mA cm^{-2}. To define the effect of the pulse sequence on the magnetic properties of the deposits, we recorded Mössbauer spectra and hysteresis loops with samples prepared as described below.

3.1. *Mössbauer spectra obtained with a short time pulse (0.1 s)*

Figure 4 shows an example of such spectra. The width of the peaks makes the acquisition of good quality spectra difficult. The signal/background ratio is weak and limits the precision of the results. The fitting of the spectral data to the classical sextuplet of metallic iron is, in our case, inadequate. The best adjustment is obtained with four Lorentz curves yielding two peaks at +5.0 mm s^{-1} and –5.0 mm s^{-1} with the same area and

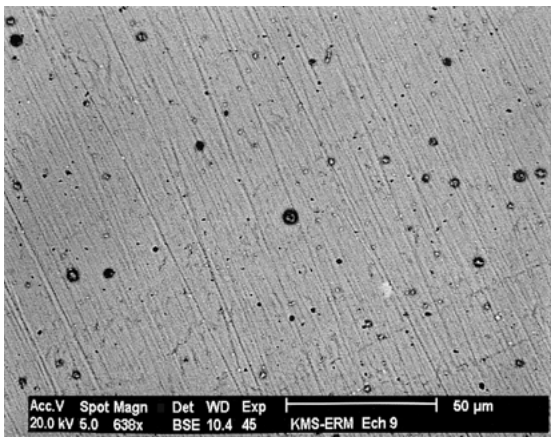

Fig. 3. Deposit obtained on copper (SEM/EDXA analysis). Current density: 30 mA cm^{-2}. Pulse 0.1 s (on)–1 s (off). Bath: $FeCl_2$ 0.06 M, $DyCl_3$ 0.04 M in formamide. The laminating effect on the bare copper substrate is still perceptible as parallel lines.

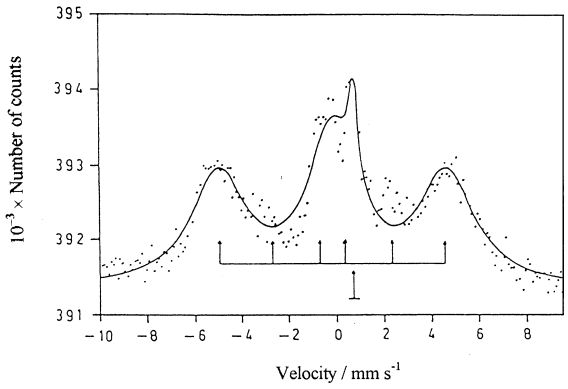

Fig. 4. Mössbauer spectrum obtained with a short electrolysis time (time on): 0.1 s. Current density: 50 mA cm^{-2}. Pulse 0.1 s (on)–1 s (off). Bath: $FeCl_2$ 0.06 M, $DyCl_3$ 0.04 M in formamide. Substrate: Cu. Experimental Mössbauer parameters at room temperature: first subspectrum (HI) = 29.6 ± 0.6 T, (IS) = −(0.04 ± 0.08) mm s^{-1}; second subspectrum (IS) = −(0.64 ± 0.05) mm s^{-1}.

width, and two interpenetrating peaks at 0.0 mm s^{-1} and 0.6 mm s^{-1}.

Our interpretation involves the contribution of two phases in the spectrum. Three peaks are attributed to the first phase: $v = -5.0$, 0.0, $+5.0$ mm s^{-1} and the fourth one at $+0.6$ mm s^{-1} to the second phase.

3.1.1. *Phase 1*

The three peaks are attributed to magnetic hyperfine interactions in αFe ($v = -5.0$, 0.0, $+5.0$ mm s^{-1}). The magnitude of the measured hyperfine field (HF) associated with these peaks is 29.6 ± 0.6 T and the measured associated isomeric shift (IS) is $-(0.04 \pm 0.08)$ mm s^{-1}. These values are comparable to the reference values for α-Fe, 33 T and 0.0 mm s^{-1}, respectively [11]. We thus suggest the presence of metallic iron in the deposit.

As mentioned above, the typical sextuplet with intensity ratios 3;2;1;1;2;3 of the Mössbauer lines is not found. The absence of peaks 2 and 5 could be due to a polarization effect. In this case, a preferential magnetization direction of the deposit perpendicular to the substrate plane leads to attenuation of these peaks [1]. Moreover, the width of the peaks may indicate a relaxation effect associated with very thin particles of metal. If we compare our spectra with computed relaxation spectra [13], we conclude that the relaxation time lies between 2.5×10^{-9} s and 5.0×10^{-9} s, corresponding to particle sizes lower than 3 nm in diameter [14].

3.1.2. *Phase 2*

The second phase contributes to the spectrum as a single peak which, with a value of 0.6 ± 0.1 mm s^{-1}, is characteristic of an isomeric shift. The presence of $FeCl_2$ ($IS = 1.4 \pm 0.1$ mm s^{-1}) [11] or FeO ($IS = 1.3 \pm 0.1$ mm s^{-1}) [16] can be dismissed. The magnetic oxides Fe_2O_3 ($HF = 51.4 \pm 0.2$ T) [11] and $DyFeO_3$ ($HF = 49.5 \pm 0.2$ T) [17], which display a magnetic spectrum with peaks at velocity higher than 8 mm s^{-1}, are absent in our data. Tentatively we associate this spectrum to a nonmagnetic Dy/Fe alloy.

Thus, the spectra of samples resulting from short electrolysis pulses are satisfactorily described as arising from the simultaneous presence of small particles of magnetic metallic iron probably oriented perpendicular to the sample plane and of a non magnetic Dy/Fe alloy.

3.2. *Mössbauer spectra obtained with long time pulses (1 s)*

As examplified by Figure 5, the magnetic behaviour of such deposits also suggests the presence of two subspectra. Here, we find a sextuplet also found in metallic iron. The hyperfine parameters obtained with the Lorentz adjustment indicate that the magnitude of the experimental hyperfine magnetic field is 34.4 ± 0.2 T and that the experimental isomeric shift is $-(0.04 \pm 0.06)$ mm s^{-1}. As discussed above, these values are characteristic of α-Fe. Sextuplet components are

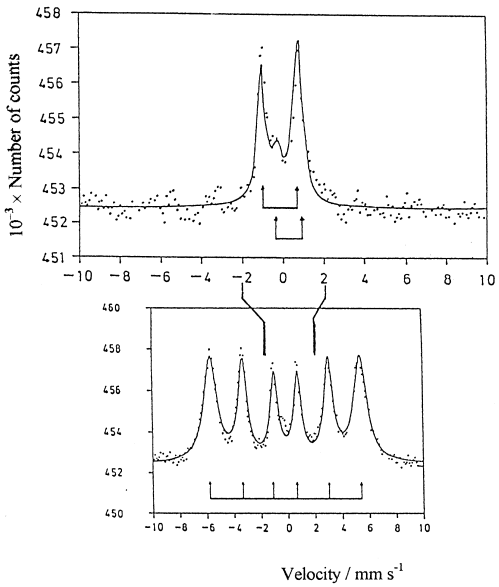

Fig. 5. Mössbauer spectrum obtained with a long electrolysis time (time on): 1 s. Current density: 50 mA cm^{-2}. Pulse 0.1 s (on)–1 s (off). Bath: $FeCl_2$ 0.06 M, $DyCl_3$ 0.04 M in formamide. Substrate: Cu. Experimental Mössbauer parameters at room temperature: first subspectrum (HI) = 34.4 ± 0.2 T, $G_{0.5}$ (1–6) = 0.60 ± 0.04 mm s^{-1}, (IS) = −(0.04 ± 0.06) mm s^{-1}; second subspectrum (QS) = 0.85 ± 0.03 mm s^{-1}, (IS) = 0.42 ± 0.05 mm s^{-1}.

broad: the half-line width at half-height ($G_{0.5}$) is 0.60 ± 0.04 mm s^{-1} for the two external lines. This width is proportional to the line shift related to the zero velocity $G_{0.5}$ (2–5) = 0.39 ± 0.04 mm s^{-1} and $G_{0.5}$ (3–4) = 0.34 ± 0.04 mm s^{-1}. This pattern is characteristic of a hyperfine field distribution, suggesting the presence of a metallic iron phase.

A better fit of the spectrum is obtained by adding to the sextuplet between –2.0 and +2.0 mm s^{-1} a doublet of two identical lines (Quadrupole splitting (QS) = 0.82 ± 0.03 mm s^{-1} and $IS = 0.42 \pm 0.05$ mm s^{-1}). The presence of $FeCl_2$ ($QS = 0.5 \pm 0.1$ mm s^{-1}) [15], $FeCl_3$ ($QS = 0.05 \pm 0.02$ mm s^{-1}) [15], FeO ($QS = 0.3 \pm 0.1$ mm s^{-1}) [17] and Fe_2O_3 ($QS = 0.09 \pm 0.02$ mm s^{-1}) [11] can be disregarded. We tentatively conclude the presence of a second non magnetic phase.

It seems that long electrolysis pulses lead to a predominant magnetic phase including different sized particles responsible for the hyperfine field distribution. This phase is likely to be metallic iron. We attribute a second phase indicated by the second subspectrum to a nonmagnetic compound composed of Fe and Dy.

For $t_{on} = 0.1$ s, the hysteresis loops reveal the typical profile of a ferromagnetic material. Figure 6 illustrates the loop obtained for a layer deposited on Au ($j = 50$ mA cm^{-2}); the pulse sequence is 0.1 s (on)–1 s (off)). Results compiled in Table 2 indicate a complicated influence of the electrolytic parameters on the coercive field and the magnetization. The mass of the deposits were obtained by ICP measurements after dissolution in HNO_3. The saturation field was calculated after standardization of the magnetometer by a

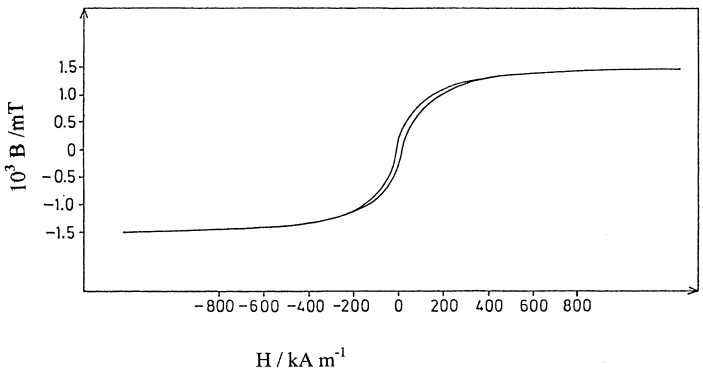

Fig. 6. Hysteresis loop recording. Substrate: Au. Current density: 50 mA cm^{-2}. Pulse 0.1 s (on)–1 s (off). Saturation: 1.51×10^{-4} mT (1.51×10^{-3} G) (deposited mass 0.002 g). Coercive field: 15.91 kA m^{-1} (200 G).

Table 2. Results obtained from hysteresis loop recordings

Current density /mA cm^{-2}	Pulse sequence /s	Coercive field /kA m^{-1}	$10^3\times$ Saturation /mT	Deposited mass /g
30	0.1(on)–1(off)	11.13 (140G)	1.31	0.005
40	0.1(on)–1(off)	3.98 (50G)	1.24	0.004
50	0.1(on)–1(off)	15.91 (200G)	1.51	0.002

Bath: $FeCl_2$ 0.06 M, $DyCl_3$ 0.04 M in formamide. Substrate: Au.

Ni sphere of 0.1500 g, the specific saturation field of Ni at room temperature being reported as 54.39 G g^{-1} [18].

The most interesting result is observed for the deposit prepared at 50 mA cm^{-2}. The coercive field is 15.91 kA m^{-1} and the saturation is 1.51×10^{-3} mT for a deposited mass of 0.002 g. This corresponds to the highest incorporation of the rare earth in the layer. The main contribution is, nevertheless, due to iron which constitutes at least 90 at % of the deposit.

The faradic yields calculated from these values are similar to those calculated for the deposition of Fe from $FeCl_2$ for 20 mA cm^{-2} $\leqslant j \leqslant$ 50 mA cm^{-2} (Cu cathode) and were found to be 99% at 20 mA cm^{-2} and 23% at 50 mA cm^{-2}. This clearly indicates that the reduction of the solvent is proportional to the current density.

4. Conclusions

The experimental results demonstrate the usefulness of Mössbauer spectroscopy for the characterization of thin magnetic layers in terms of structure and magnetic properties. With the highest current density used (50 mA cm^{-2}), the results suggest the presence of two phases in the deposits. One of these phases is probably metallic magnetic iron and the second is attributable to a Dy/Fe alloy. Evidence of a perpendicular magnetization to the surface plane, in the case of a short electrolysis pulses ($t_{on} = 0.1$ s), is very important with regard to the preparation of magnetooptic memories. Complementary data are gained when comparing SEM/EDXA and Mössbauer results.

From an electrochemical point of view, the formation of small particles with random orientation is facilitated by a current density near to the limiting diffusion current [19]. A short cathodic current application favours nucleation with respect to grain growth.

Coercive field values are smaller than those described in the literature for samples prepared by sputtering or evaporation. The probable reason is that our deposits do not consist of stoichiometrically well defined crystalline structures. Different kinds of partially amorphous structures may appear and detrimentally influence the coercive force.

Acknowledgements

We thank the Inter-University Institute for Nuclear Sciences (IISN) for support of this work.

References

1. K.H.J. Buschow, G.J. Long and F.Grandjean, 'High Density Digital Recording', NATO ASI Series, Serie E: Applied Sciences, Vol. 229, (1994).
2. J.M. Cadogan, *J. Phys. D: Appl. Phys.* **29** (1996) 2246.
3. C.E. Johnson, *J. Phys. D: Appl. Phys.* **29** (1996) 2266.
4. Y. Sakurai and K. Saiki, Perpendicular Magnetization Film and its Production. *European Patent 0 164 725 B1* (1989).
5. U. Kullman, E. Koester and C. Dorsch, *IEEE Trans. Magn.* **MAG-20**(2) (1994) 420–424.
6. Y. Sato, H. Ishida, K. Kobayakawa and Y. Abe, *Chem. Lett.* (1990) 1471–1474.
7. Y. Matsuda, T. Fujii, N. Yoshimoto and M. Morita, *J. Alloys Compd.* **193** (1993) 23–25.
8. Y. Sato, T. Takazawa, M. Takahashi, H. Ishida and K. Kobayakawa, *Plat. Surf. Finish.* (1993) 72–74.

9. N. Usuzaka, H. Yamaguchi and T. Watanabe, *Mater. Sci. Eng.* **99** (1988) 105–108.
10. D. Leroy, L. Martinot, C. Licour, C. Jérome, H. Zhan and D. Strivay, *J. Chim. Phys.* **95** (1998) 1491–1493.
11. A. Muir, K. Ando and H. Coogan, '*Mössbauer Effect Data Index 1958–1965*', (Interscience Publishers, New York, 1965).
12. N. Holstein and K. Jüttner, *Electrochemical Society Proceedings*, Vol. **97-27** pp. 240–251.
13. A.J. Dekker, '*Hyperfine Interactions*' (Academic Press, NewYork, 1967).
14. H. Herpin, '*Théorie du Magnétisme*' (Presses universitaires de France, Paris, 1968).
15. G.K. Wertheim and J.H. Wernick, *Phys. Rev.* **125** (1962) 1937–1940.
16. M. Eibschutz, G. Gorodetsky, S. Shtrikman and D. Treves, *J. Appl. Phys.* **35** (1964) 1071–1072.
17. G. Shirane, D. Cox and S. Ruby, *Phys. Rev.* **125** (1962) 1158–1165.
18. 'Handbook of Chemistry' (CRC Press, Boca Raton 60th edn, 1979).
19. R. Winand, *Electrochim. Acta.* **39** (1994) 1091–1105.